

# Multirate Repetitive Control and Applications

– Verification of Switching Scheme by HDD and Visual Servoing –

Hiroshi Fujimoto<sup>†‡</sup> Fumihiro Kawakami<sup>‡</sup> Seiji Kondo<sup>‡</sup>

<sup>†</sup>School of Mechanical Engineering, Purdue University

West Lafayette, IN 47907-1288, [hfuji@ieee.org](mailto:hfuji@ieee.org)

<sup>‡</sup>Department of Electrical Engineering, Nagaoka University of Technology, Japan

## Abstract

In this paper, two multirate repetitive controllers are proposed, namely, repetitive intersample disturbance rejection (RIDR) and repetitive perfect tracking control (RPTC). First, in order to develop RIDR, multirate intersample disturbance rejection algorithm is reviewed which was proposed by authors for general digital control systems with restricted sampling frequency. Second, RPTC method is proposed to reduce the computation cost for system with many disturbance modes, in which the multirate control is introduced to overcome unstable zero problem of discrete-time plant. Third, both for RIDR and RPTC, the novel scheme of repetitive feedforward control is proposed based on switching mechanism, which enables the rejection of periodical disturbance without any sacrifice of the closed-loop characteristics. Finally, the proposed methods are applied to high-order repeatable runout (RRO) rejection problem of hard disk drive (HDD) and high-speed motion tracking problem of visual servoing. The advantages and disadvantages of these approaches are demonstrated through simulations and experiments.

## 1 Introduction

Repetitive control is a widely used technique to reject periodic disturbances [1, 2]. Although this control scheme has excellent performance for low order disturbance modes, it is very difficult to reject relatively higher frequency modes. The reasons of this difficulty are 1) the delay caused by zero-order hold of plant input when the high-order disturbance is close to Nyquist frequency, 2) the low-pass filter is required to assure the stability robustness, and 3) approximated inverse is implemented because of the unstable zero of discrete-time plant [3] in the conventional discrete-time repetitive controller [1]. In this paper, these problems are resolved by introducing novel control schemes.

A digital control system generally has the sampler  $\mathcal{S}$  of sensor output  $y(t)$  and the holder  $\mathcal{H}$  of control input  $u(t)$ , as shown in Fig. 1. The recent development of computer technology enabled to set the control period  $T_u$  shorter than the sampling period  $T_y$  when the sensor speed is restricted. In this paper,

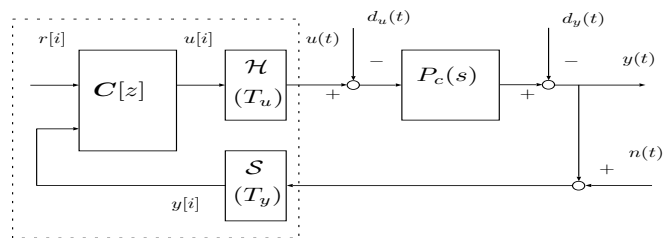
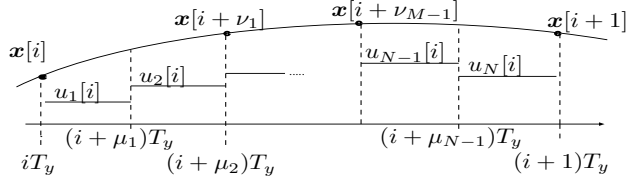


Figure 1: Digital control system.

the above-mentioned first problem of holder delay is overcome by introducing repetitive intersample disturbance rejection (RIDR) using the multirate input control ( $T_u < T_y$ ). Especially in head-positioning systems of hard disk drives [4, 5] and visual servo systems of robot manipulators [6], the multirate input control has great advantages since the sampling period of sensor signal is restricted to be long by the number of servo signals and the video rate of camera, respectively.

In the conventional repetitive control [1], the discrete-time disturbance model  $(z^{N_d} - 1)^{-1}$  is implemented in feedback controller as the internal model. Although the sensitivity function becomes zero at the disturbance frequencies  $k\omega_d$ , the sensitivity has big amplitude at the other frequency band, which causes severe damage in total tracking accuracy. Moreover, the closed-loop system could become unstable because the peak gain of internal model excites the unmodeled dynamics. Therefore, low-pass filter is usually implemented in repetitive control to assure the stability robustness at the sacrifice of high-frequency disturbance rejection performance. On the other hand, this paper introduces novel switching schemes to achieve repetitive disturbance rejection by feedforward control.

The third problem of discrete-time unstable zero was not crucial in the conventional feedback repetitive control because the stability can be assured even when the approximated zero-phase-error (ZPE) inverse is utilized [1]. However, when the feedforward scheme is introduced with switching scheme, the gain characteristics of ZPE [7] causes the tracking error especially for high-order disturbance. Therefore, in the proposed RPTC scheme, the perfect tracking control which was proposed by authors in [8] is implemented using multirate



**Figure 2:** Multirate sampling control.

input control to obtain the ideal inner-loop system in discrete-time domain.

## 2 Intersample Disturbance Rejection Control

In this section, the intersample disturbance rejection control which was proposed by authors in [4, 9] is briefly reviewed. For simplification, the plant is assumed to be a single-input single-output system. The proposed methods, however, can be extended to deal with the multi-input multi-output system [10, 11].

In the proposed multirate scheme, it is assumed that the control period  $T_u$  can be set  $N$  times shorter than the sampling period of plant output  $T_y (= NT_u)$ . The plant state variable  $\mathbf{x}$  is evaluated  $M := N/n$  times during one sampling period, where  $n$  is the plant order.

In Fig. 2,  $\mu_j (j = 0, 1, \dots, N)$  and  $\nu_k (k = 1, \dots, M)$  are parameters for the timing of input changing and state evaluation, which satisfy the following conditions.

$$0 = \mu_0 < \dots < \mu_N = 1, \quad 0 < \nu_1 < \dots < \nu_M = 1 \quad (1)$$

If  $T_y$  is divided at equal intervals, the parameters are set to  $\mu_j = j/N$ ,  $\nu_k = k/M$ , and  $T_u = (\mu_j - \mu_{j-1})T_y$ .

### 2.1 Plant discretization by multirate sampling

Consider the continuous-time plant described by

$$\dot{\mathbf{x}}(t) = \mathbf{A}_c \mathbf{x}(t) + \mathbf{b}_c u(t), \quad y(t) = \mathbf{c}_c \mathbf{x}(t). \quad (2)$$

The discrete-time plant discretized by the multirate sampling control of Fig. 2 becomes

$$\mathbf{x}[i+1] = \mathbf{A} \mathbf{x}[i] + \mathbf{B} \mathbf{u}[i], \quad y[i] = \mathbf{c} \mathbf{x}[i], \quad (3)$$

where  $\mathbf{x}[i] = \mathbf{x}(iT)$ , and where  $\mathbf{A}$ ,  $\mathbf{B}$ ,  $\mathbf{c}$ , and  $\mathbf{u}[i]$  are given by

$$\begin{bmatrix} \mathbf{A} & \mathbf{B} \\ \mathbf{c} & \mathbf{O} \end{bmatrix} := \begin{bmatrix} e^{\mathbf{A}_c T_y} & \mathbf{b}_1 & \dots & \mathbf{b}_N \\ \mathbf{c}_c & 0 & \dots & 0 \end{bmatrix}, \quad (4)$$

$$\mathbf{b}_j := \int_{(1-\mu_j)T_y}^{(1-\mu_{j-1})T_y} e^{\mathbf{A}_c \tau} \mathbf{b}_c d\tau, \quad \mathbf{u}[i] := [u_1[i], \dots, u_N[i]]^T. \quad (5)$$

### 2.2 Intersample disturbance rejection (IDR)

To design the intersample disturbance rejection control, consider the continuous-time plant described by

$$\dot{\mathbf{x}}_p(t) = \mathbf{A}_{cp} \mathbf{x}_p(t) + \mathbf{b}_{cp}(u(t) - d(t)), \quad y(t) = \mathbf{c}_{cp} \mathbf{x}_p(t), \quad (6)$$

where  $d(t)$  is the disturbance input. Let the disturbance model be

$$\dot{\mathbf{x}}_d(t) = \mathbf{A}_{cd} \mathbf{x}_d(t), \quad d(t) = \mathbf{c}_{cd} \mathbf{x}_d(t). \quad (7)$$

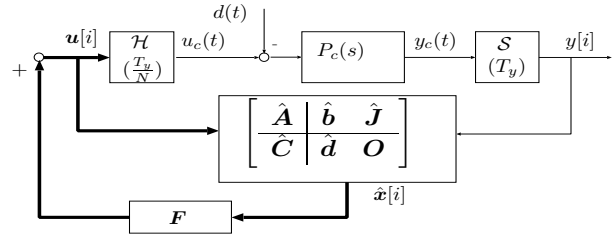


**Figure 3:** Multirate control with disturbance observer.

For example, step type disturbance can be modeled as  $\mathbf{A}_{cd} = 0$ ,  $\mathbf{c}_{cd} = 1$  and sinusoidal type disturbance with frequency  $\omega_d$  can be modeled as

$$\mathbf{A}_{cd} = \mathbf{A}_\omega(\omega_d) := \begin{bmatrix} 0 & 1 \\ -\omega_d^2 & 0 \end{bmatrix}, \quad \mathbf{c}_{cd} = [1, 0]. \quad (8)$$

The continuous-time augmented system consisting of (6) and (7) is represented by (2) where

$$\mathbf{A}_c := \begin{bmatrix} \mathbf{A}_{cp} & -\mathbf{b}_{cp} \mathbf{c}_{cd} \\ \mathbf{O} & \mathbf{A}_{cd} \end{bmatrix}, \quad \mathbf{b}_c := \begin{bmatrix} \mathbf{b}_{cp} \\ \mathbf{0} \end{bmatrix}, \quad (9)$$

$$\mathbf{c}_c := [\mathbf{c}_{cp}, \mathbf{0}], \quad \mathbf{x} := [\mathbf{x}_p^T, \mathbf{x}_d^T]^T. \quad (10)$$

The intersample plant state at  $t = (i + \nu_k)T_y$  is represented by

$$\tilde{\mathbf{x}}_p[i + \nu_k] = \tilde{\mathbf{A}}_{pk} \mathbf{x}_p[i] + \tilde{\mathbf{E}}_k \mathbf{x}_d[i] + \tilde{\mathbf{B}}_{pk} \mathbf{u}[i], \quad (11)$$

where the coefficient matrices are defined in [4, 9].

For the discrete-time plant (3) with (9), the estimated state  $\hat{\mathbf{x}} = [\hat{\mathbf{x}}_p^T, \hat{\mathbf{x}}_d^T]^T$  can be obtained at sampling point through observer, as shown in Fig. 3. Then, let the feedback control law be

$$\mathbf{u}[i] = \mathbf{F}_p \hat{\mathbf{x}}_p[i] + \mathbf{F}_d \hat{\mathbf{x}}_d[i] := \mathbf{F} \hat{\mathbf{x}}[i]. \quad (12)$$

From (11) and (12), the closed-loop system is represented by

$$\mathbf{x}_p[i + \nu_k] = \tilde{\mathbf{A}}_{Fpk} \mathbf{x}_p[i] + (\tilde{\mathbf{E}}_k + \tilde{\mathbf{B}}_{pk} \mathbf{F}_d) \mathbf{x}_d[i] + \tilde{\mathbf{B}}_{pk} \mathbf{F} \mathbf{e}[i],$$

where  $\tilde{\mathbf{A}}_{Fpk} := \tilde{\mathbf{A}}_{pk} + \tilde{\mathbf{B}}_{pk} \mathbf{F}_p$  and  $\mathbf{e}[i] := \hat{\mathbf{x}}[i] - \mathbf{x}[i]$ . The matrix gain  $\mathbf{F}_d$  is selected so that the second term of above right side becomes zero for all  $k = 1, \dots, M$  as

$$\mathbf{F}_d = -\tilde{\mathbf{B}}_p^{-1} \tilde{\mathbf{E}}. \quad (13)$$

The full rank of  $\tilde{\mathbf{B}}_p$  is assured in [12]. Thus the influence from disturbance  $\mathbf{x}_d[i]$  to the intersample state  $\mathbf{x}_p[i + \nu_k]$  becomes zero. Moreover,  $\mathbf{x}_p[i]$  and  $\mathbf{e}[i]$  converge to zero if  $\tilde{\mathbf{A}}_{pM} + \tilde{\mathbf{B}}_{pM} \mathbf{F}_p$  and  $\tilde{\mathbf{A}}$  (the regulator and observer) are stable [4, 9]. Therefore, perfect disturbance rejection is achieved ( $\mathbf{x}_p[i + \nu_k] = 0$ ) in the steady state. The poles of the regulator and observer should be tuned by taking account of the tradeoff between the performance and stability robustness.

In this paper, the number  $M$  is fixed to  $N/n$  in order to reject the disturbance perfectly at  $M$  inter-sample points. On the other hand,  $M$  can be selected more than  $N/n$  to optimize the whole inter-sample perfor-

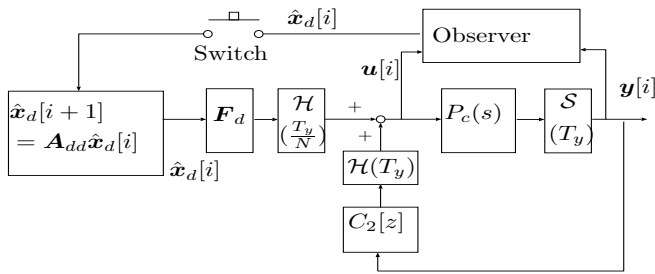


Figure 4: Feedforward RIDR control.

mance [9] in the same way as modern sampled-data theory [13].

### 3 Multirate Repetitive Controllers

#### 3.1 Repetitive intersample disturbance rejection (RIDR)

In this section, the proposed intersample disturbance rejection control is applied to periodic disturbance [9]. The disturbance with period  $T_d := 2\pi/\omega_d$  can be represented by the Fourier series as

$$d(t) = a_0 + \sum_k a_k \cos k\omega_d t + b_k \sin k\omega_d t. \quad (14)$$

where  $\omega_d$  is known and  $a_0, a_k,$  and  $b_k$  are unknown parameters. Because the index  $k$  can be selected freely, the disturbance mode with large power spectrum should be modeled from experimental analysis. By letting the disturbance model (7) be (15), the repetitive disturbance is perfectly rejected ( $\mathbf{x}_p[i + \nu_k] = 0$ ) at  $M$  inter-sample points in the steady state.

$$\mathbf{A}_{cd} = \text{diag}\{0, \mathbf{A}_\omega(\omega_d), \dots, \mathbf{A}_\omega(k\omega_d), \dots\} \quad (15)$$

$$\mathbf{c}_{cd} = [1, 1, 0, \dots, 1, 0, \dots] \quad (16)$$

However, the repetitive feedback control based on the internal model principle has disadvantages that closed-loop characteristics worsen and it becomes difficult to assure stability robustness [14]. Therefore, in this section, a novel repetitive controller based on open-loop estimation with switching mechanism and feedforward disturbance rejection is proposed, as shown in Fig. 4 [9].

The repetitive disturbance is estimated by the open-loop disturbance observer based on (14). When the estimation converges to the steady state, the switch turns on at  $t = t_{sw}$ . After that, the switch turns off immediately. Repetitive disturbance is calculated by (17) from the initial value  $\hat{\mathbf{x}}_d[t_{sw}]$  which contains the amplitude and phase information of the disturbance.

$$\hat{\mathbf{x}}_d[i + 1] = \mathbf{A}_{dd}\hat{\mathbf{x}}_d[i], \quad \mathbf{A}_{dd} = \exp(\mathbf{A}_{cd}T_y) \quad (17)$$

Because the disturbance feedforward  $\mathbf{F}_d$  is obtained by (13), perfect disturbance rejection is achieved at  $M$  inter-sample points. The advantage of this approach is that the feedback controller  $C_2[z]$  is completely independent of the repetitive controller. Thus stability robustness is guaranteed by the feedback controller ob-

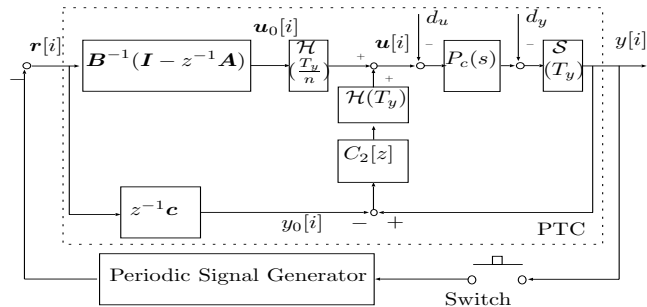


Figure 5: Repetitive perfect tracking controller.

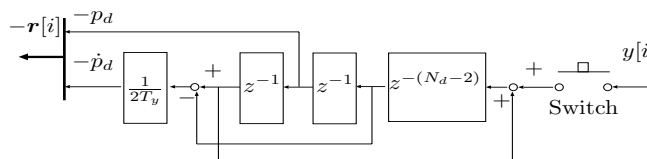


Figure 6: Periodic signal generator for 2nd order system.

tained from robust control theory. With this scheme, it becomes possible to construct the repetitive controller without sacrifice of the feedback characteristics. In Fig. 4, the  $C_2[z]$  is assumed to be a single-rate controller with  $T_y$ . However, multirate feedback controller is also available to recover the phase-delay generated by zero-order hold [5, 15].

#### 3.2 Repetitive perfect tracking control (RPTC)

In the above RIDR method, the observer estimates periodic disturbance based on the disturbance model (14). Although this model has diagonal structure (15), the on-line computation cost will become high if many disturbance modes are selected. In this section, a novel repetitive control scheme is proposed based on perfect tracking controller (PTC) [5, 8] with periodic signal generator (PSG). Because the PSG can be constructed by the series of  $z^{-1}$ , the computation cost is very low [16].

First, the perfect tracking controller is designed using multirate feedforward control [8] as minor-loop system to obtain the desired command response  $z^{-1}\mathbf{I}$ . The input multiplicity is fixed to the plant order  $N = n$ . The measured output  $y[i]$  of (3) is modified using discrete-time disturbance  $d[i]$  as

$$y[i] = p[i] - d[i] := \mathbf{c}\mathbf{x}[i] - d[i], \quad (18)$$

where  $p[i]$  and  $\mathbf{x}[i]$  are the plant output and state, respectively. From (3), the transfer function from  $\mathbf{x}[i + 1] \in \mathbf{R}^n$  to the multirate input  $\mathbf{u}[i] \in \mathbf{R}^n$  is described by

$$\mathbf{u}[i] = \mathbf{B}^{-1}(\mathbf{I} - z^{-1}\mathbf{A})\mathbf{x}[i + 1]. \quad (19)$$

In (19), the nonsingularity of matrix  $\mathbf{B}$  is assured for controllable plant in case of  $N = n$  [12]. Because all poles of the transfer function (19) are zero, it is found that (19) is a stable inverse system. Thus, if the control

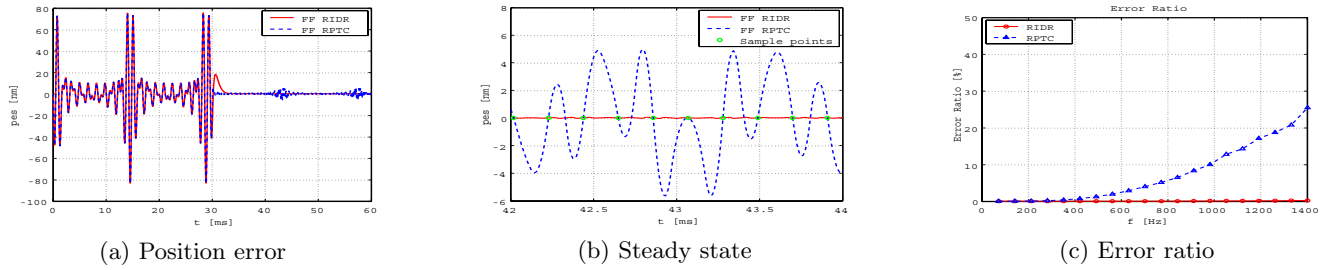


**Figure 7:** Simulation results of HDD. (Feedforward RIDR vs. Feedforward RPTC)

input is calculated by (20) as shown in Fig. 5, perfect tracking is guaranteed at sampling points [8] because (20) is the exact inverse plant.

$$\mathbf{u}_0[i] = \mathbf{B}^{-1}(\mathbf{I} - z^{-1}\mathbf{A})\mathbf{r}[i] \quad (20)$$

Here,  $\mathbf{r}[i](:= \mathbf{x}_d[i + 1])$  is previewed desired trajectory of plant state. The output of the nominal plant without disturbance can be calculated by

$$y_0[i] = \mathbf{c}\mathbf{x}_d[i] = z^{-1}\mathbf{c}\mathbf{r}[i]. \quad (21)$$

When the tracking error  $y[i] - y_0[i]$  is caused by disturbance or modeling error, it can be eliminated using the robust feedback controller  $C_2[z]$ , as shown in Fig. 5.

Second, the periodic signal generator is designed to generate desired trajectory  $\mathbf{r}[i]$ . Because perfect tracking ( $\mathbf{x}[i] = \mathbf{x}_d[i]$  or  $\mathbf{x}[i] = z^{-1}\mathbf{I}_n\mathbf{r}[i]$ ) is assured, the minor-loop system is expressed as

$$y[i] = z^{-1}r[i] - d_2[i], \quad r[i] := \mathbf{c}\mathbf{r}[i], \quad (22)$$

where  $d_2[i] := (1 - P[z]C_2[z])^{-1}d[i]$  and  $P[z]$  is the single-rate plant with  $T_y$ . In the same way as section 3.1, both the feedback and feedforward approaches can be considered in this RPTC scheme. In case of feedback scheme, the switch of Fig. 5 is always on-state. The PSG can be designed as the outer-loop controller by

$$r[i] = -\frac{z}{z^{N_d} - 1}y[i], \quad (23)$$

where integer  $N_d$  is defined as  $T_d/T_y$ . From (22) and (23), the total closed-loop system is represented by

$$y[i] = -\frac{z^{N_d} - 1}{z^{N_d}}d_2[i] \quad (24)$$

Therefore, the repetitive disturbance which is modeled as  $d[i] = (z^{N_d} - 1)^{-1}$  is completely rejected at every sampling point in steady-state.

In (22), there is redundancy to decide  $\mathbf{r}[i] \in \mathbf{R}^n$  from the PSG output  $r[i]$ . This issue was discussed in [17] to make the multirate input smooth. Fig. 6 shows one example of the 2nd order plant with state variable  $\mathbf{x} = [p, \dot{p}]$ , in which the velocity command is generated by  $\dot{p}_d[i] = (p_d[i + 1] - p_d[i - 1])/2T_y$ .

However, the internal model (23) damages the closed-loop characteristics such as stability robustness since the gain of PSG becomes infinity at high order har-

monics  $k\omega_d$ . Therefore, the feedforward algorithm of RPTC with switching mechanism is proposed as in section 3.1. The switch of Fig. 5 turns on during one disturbance period  $T_d$  in the steady-state after the transient of minor feedback loop with  $C_2[z]$  and  $P_c(s)$ . By using the stored signal, the PSG can reproduce the feedforward signal  $\mathbf{r}[i]$  unless the disturbance changes suddenly. Therefore, the disturbance can be rejected at every sampling point without sacrifice of the feedback characteristics.

## 4 Applications

### 4.1 RRO rejection for HDD

In the servo systems of hard disk drives (HDDs), the head position is detected by the discrete servo signals embedded in the disks. Therefore, the output sampling period  $T_y$  is decided by the number of these signals and the rotational frequency of the spindle motor. However, it is possible to set the control period  $T_u$  shorter than  $T_y$  because of the recent development of CPU. Thus the controller can be regarded as the multirate system which has the hardware restriction of  $T_u < T_y$ .

In the following mode of HDD, two kinds of disturbance at the plant output should be considered; repeatable runout (RRO) and non-repeatable runout (NRRO). While RRO is synchronous with the disk rotation, NRRO is not synchronous. Although there are many techniques to reject the RRO in low frequency region [16], the high frequency RRO is very difficult to be rejected by conventional technologies. However, the effect of high-order RRO cannot be neglected since the required servo accuracy is getting drastically severe. Therefore, this paper applies the proposed multirate repetitive controllers both of RIDR and RPTC with switching mechanism.

The plant is a 2.5-in prototype HDD which is modeled as double integrator system. The track pitch is 450[nm]. The sampling period of this drive is  $T_y = 210.08 [\mu s]$ , and the control input can be changed  $N = 4$  times during this period. In the RIDR, it is possible to select the disturbance mode  $k$  to be rejected. From the experimental analysis of position error signal (PES), the low order RRO under  $k = 9$  can be rejected well by the feedback controller  $C_2[z]$  except for

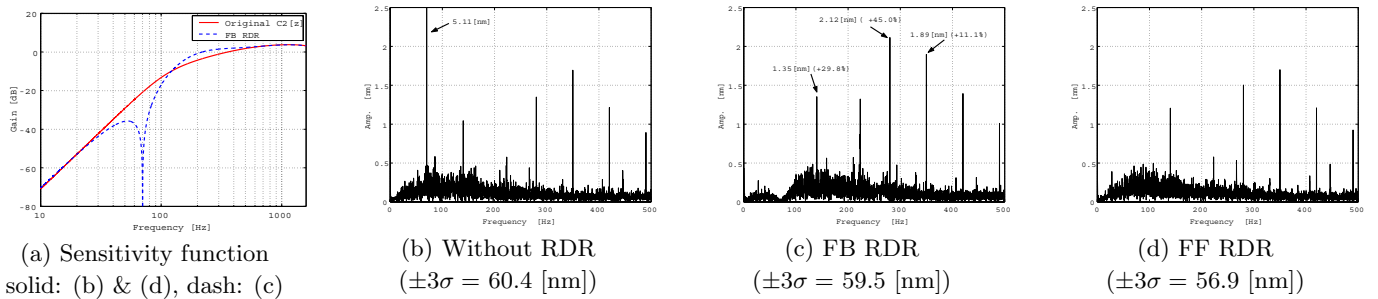


**Figure 8:** Experimental results of HDD. (Feedforward vs. Feedback Repetitive Disturbance Rejection (RDR))

the basic frequency  $k = 1$  (70 [Hz]). However, high order RRO has strong spectrum in  $k = 10 \sim 17$  (700  $\sim$  1190 [Hz]) since these region is over the cutoff frequency of  $C_2[z]$ . Therefore, the disturbance is modeled as  $k = 1, 10 \sim 17$  in RIDR.

Fig. 7 shows the simulation results of RIDR and RPTC, in which feedforward approaches are utilized with switching scheme. The amplitude of RRO is set to 20 [nm] for  $k = 1$  and 6 [nm] for  $k = 10 \sim 17$ . As shown in Fig. 7(a) and (b), the disturbance is perfectly rejected at every sampling point after the switching action  $t_{sw} = 30$  [ms]. The disturbance rejection performance of RPTC must be better than the conventional repetitive controller [1] since it does not need the low-pass filter. In spite of that, the intersample response of RIDR is much smaller than that of RPTC. The disturbance rejection is assured only at sampling points in RPTC because discrete-time disturbance model  $(z^{N_d} - 1)^{-1}$  is utilized. On the other hand in RIDR, intersample disturbance rejection of state variable is guaranteed based on the continuous model (14). Thus the position error and its derivative becomes zero at  $M (= N/n = 4/2 = 2)$  intersample points in steady-state.

Fig. 7c shows evaluated results of the error ratio  $E(k)$  for the disturbance order  $k$ . Considering the intersample response, the error ratio is numerically calculated in simulation by

$$E^2(k) := \frac{\int_{t_s}^{t_s+kT_d} y(t)^2 dt}{\int_{t_s}^{t_s+kT_d} d_y(t)^2 dt}, \quad (25)$$

where the runout is given by  $d_y(t) = \sin k\omega_d t$ ,  $y(t)$  is the position error, and  $t_s$  is selected as  $t_{sw} + 10$  [ms] in order to evaluate the steady state. In the high frequency region close to the Nyquist frequency (2.4 [kHz]), intersample disturbance rejection performance of RIDR is much better than that of RPTC.

However, from the point of view of computation cost, RPTC is superior to RIDR. Because the disturbance is modeled as the 9 sinusoidal modes ( $k = 1, 10 \sim 17$ ) and 1 dc mode ( $k = 0$ ), the matrix  $A_{cd}$  has one scalar and 9 matrices of  $A_\omega \in \mathbf{R}^{2 \times 2}$  in diagonal elements as

expressed in (15). Therefore, the open-loop observer should include this matrix in discrete-time form. Note that  $\exp(A_{cd}T_y)$  still has the diagonal structure with many zero elements. In spite of that, computation cost is not negligible if many modes are modeled. On the other hand in RPTC, the periodic signal generator can be constructed by the  $N_d (= 68)$  memories, which can be realized just by pointer operator as show in Fig. 6. The order of inner-loop PTC described by (20) and (21) is the same with the plant order  $n$ .

## Experiments

Next, the feedback and feedforward schemes are compared through experiments. As a first step of experimental verification, only the basic mode  $k = 1$  is considered. Because the 70 [Hz] is far away from the Nyquist frequency, the single-rate control ( $N = 1$ ) is utilized for simplification. Then, the disturbance rejection of position error is assured at sampling points. Both the FB (Fig. 3) and FF (Fig. 4) controllers are designed by the algorithm of section 3.1.

As shown in Fig. 8a, the internal model of FB approach damages the sensitivity function in 120  $\sim$  600 [Hz] band compared with the original lead-lag controller  $C_2[z]$ . Therefore, the position error of FB approach (Fig. 8c) becomes larger than that of the original controller (Fig. 8b) in this band although the runout is rejected at 70 [Hz] and its neighborhood. On the other hand, FF approach with the original  $C_2[z]$  completely rejects 70 [Hz] mode as well as it does not effect any other frequency region, as shown in Fig. 8d. While the PES variance ( $\pm 3\sigma$ ) of FB approach is 1.49 [%] smaller than the original controller, FF approach reduces 5.79 [%] position error.

## 4.2 Visual servoing of robot manipulator

In this section, visual servo problem is considered, in which the camera mounted on the robot manipulator tracks a repetitively moving object, as shown in Fig. 9 [6]. In our experimental setup, while the sampling period of CCD camera is restricted to  $T_y = 100$  [ms], the joint servo period can be set to 1 [ms]. Thus the workspace robust controller is implemented as inner-

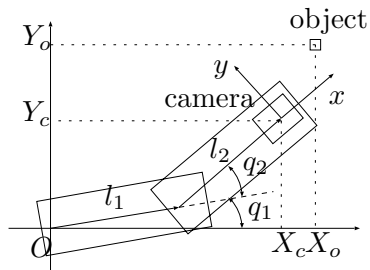


Figure 9: Two-link DD robot with camera.

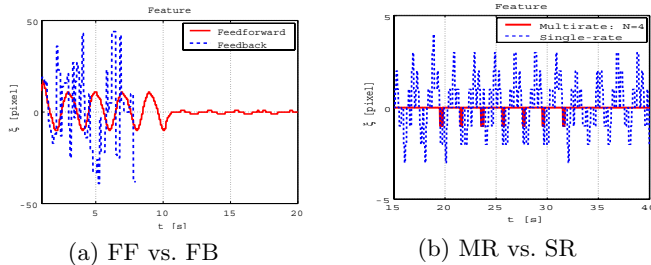


Figure 10: Experiments of visual servoing.

loop system with the short period 1 [ms]. The position command from outer vision loop is regarded as control input and the period is set to  $T_u = 25$  [ms]. By using the inverse mapping of nonlinear perspective transformation, linear diagonal plant can be obtained [6].

Both of feedforward (Fig. 4) and feedback (Fig. 3) RIDR controllers are designed for  $k = 1$ st, 3rd, and 5th order disturbances with  $\omega_d = 2\pi 0.5$  [rad/sec]. As shown in Fig. 10a, the conventional feedback repetitive controller becomes unstable because high-order internal model damages the stability robustness. On the other hand, in the proposed feedforward repetitive control, the error of the image feature converges quickly after  $t_{sw} = 10$  [s]. Fig. 10b shows the steady-state error of the multirate and single-rate controllers. Because the intersample disturbance rejection is assured, the error of multirate control is much smaller than that of single-rate control.

## 5 Conclusion

In this paper, two multirate repetitive controllers of RIDR and RPTC were proposed to reject high-order repetitive disturbances. The advantages and disadvantages of these schemes were discussed. Because RIDR assures perfect disturbance rejection at  $M$  intersample points, the intersample performance is much better than RPTC. On the other hand, the computation cost of RPTC is superior to RIDR because it can be realized by the periodic signal generator and low order perfect tracking controller. The combination of two algorithm will be a reasonable choice.

Moreover, the novel control schemes of repetitive control were proposed for RIDR and RPTC based on switching mechanism and feedforward control, which

enabled to reject periodical disturbance without any sacrifice of the feedback characteristics. The advantages of these approaches were demonstrated through simulations and experiments of HDD and visual servoing.

Finally, the authors wish to thank Professor Y. Hori of the University of Tokyo for many helpful discussions and Dr. M. Kobayashi and Mr. A. Okuyama of Hitachi, Ltd, for their collaboration.

## References

- [1] K. K. Chew and M. Tomizuka: "Digital control of repetitive errors in disk drive systems", IEEE Contr. Syst. Mag., **10**, 1, pp. 16–20 (1990).
- [2] S. Hara, Y. Yamamoto, T. Omata and M. Nakano: "Repetitive control system – a new-type servo system", IEEE Trans. Automat. Contr., **33**, pp. 659–668 (1988).
- [3] K. J. Åström, P. Hangander and J. Sternby: "Zeros of sampled system", Automatica, **20**, 1, pp. 31–38 (1984).
- [4] H. Fujimoto and Y. Hori: "High-performance servo systems based on multirate sampling control", Control Engineering Practice, **10**, 7, pp. 773–781 (2002).
- [5] H. Fujimoto, Y. Hori, T. Yamaguchi and S. Nakagawa: "Proposal of perfect tracking and perfect disturbance rejection control by multirate sampling and applications to hard disk drive control", Conf. Decision Contr., pp. 5277–5282 (1999).
- [6] H. Fujimoto and Y. Hori: "Visual servoing based on intersample disturbance rejection by multirate sampling control – time delay compensation and experimental verification –", Conf. Decision Contr., pp. 334–339 (2001).
- [7] M. Tomizuka: "Zero phase error tracking algorithm for digital control", ASME, J. Dynam. Syst., Measur., and Contr., **109**, pp. 65–68 (1987).
- [8] H. Fujimoto, Y. Hori and A. Kawamura: "Perfect tracking control based on multirate feedforward control with generalized sampling periods", IEEE Trans. Industrial Electronics, **48**, 3, pp. 636–644 (2001).
- [9] H. Fujimoto and Y. Hori: "Vibration suppression and optimal repetitive disturbance rejection control in semi-Nyquist frequency region using multirate sampling control", Conf. Decision Contr., pp. 691–700 (2000).
- [10] H. Fujimoto: "General Framework of Multirate Sampling Control and Applications to Motion Control Systems", PhD thesis, The University of Tokyo (2001). <http://pelab.nagaokaut.ac.jp/~fujimoto/>.
- [11] H. Fujimoto, A. Kawamura and M. Tomizuka: "Generalized digital redesign method for linear feedback system based on N-delay control", IEEE/ASME Trans. Mechatronics, **4**, 2, pp. 101–109 (1999).
- [12] M. Araki and T. Hagiwara: "Pole assignment by multirate-data output feedback", Int. J. Control, **44**, 6, pp. 1661–1673 (1986).
- [13] T. Chen and L. Qiu: " $H_\infty$  design of general multirate sampled-data control systems", Automatica, **30**, 7, pp. 1139–1152 (1994).
- [14] C. Smith, K. Takeuchi and M. Tomizuka: "Cost effective repetitive controllers for data storage devices", 14th IFAC World Congress, Vol. B, pp. 407–412 (1999).
- [15] T. Hara and M. Tomizuka: "Performance enhancement of multi-rate controller for hard disk drives", IEEE Trans. Magnetics, **35**, 2, pp. 898–903 (1999).
- [16] C. Kempf, W. Messner, M. Tomizuka and R. Horowitz: "Comparison of four discrete-time repetitive algorithms", IEEE Contr. Syst. Mag., **13**, 5, pp. 48–54 (1993).
- [17] H. Fujimoto, Y. Hori and A. Kawamura: "Perfect tracking control method based on multirate feedforward control", Trans. SICE, **36**, 9, pp. 766–772 (2000). (in Japanese).